H. R. Mayer, E. K. Tschegg† and S. E. Stanzl-Tschegg**

High-Cycle Torsion Fatigue of Ceramic Materials under Combined Loading Conditions (cyclic torsion and static compression)

REFERENCE Mayer, H. R., Tschegg, E. K. and Stanzl-Tschegg, S. E., **High-cycle torsion fatigue of ceramic materials under combined loading conditions (cyclic torsion and static compression)**, *Multiaxial Fatigue and Design*, ESIS 21 (Edited by A. Pineau, G. Cailletaud, and T. C. Lindley) 1996, Mechanical Engineering Publications, London, pp. 411–421.

ABSTRACT Experimental results of high-cycle fatigue tests on plain tube specimens of zirconium oxide under cyclic torsion plus superimposed static compression loading at room temperature are reported. A new time and energy saving torsional ultrasonic fatigue testing machine (loading frequency 20 kHz) has been developed and used successfully to perform fatigue loading tests. The resulting S/N curves show that superposition of small compressive loads leads to up to two decades higher numbers of cycles to fracture than pure cyclic torsional loads. Crack initiation takes place under mode I and the fracture area is inclined approximately 45° towards the specimen axis in all cases.

1 Introduction

In order to design components with acceptable lifetimes, the fatigue properties of the material used must be determined under loading conditions which simulate in-service loading as far as possible. Many machine and construction parts are multiaxially loaded. Therefore many studies on the fatigue and fracture behaviour of metallic materials under bi- and multiaxial loading conditions are reported in the literature (**1, 2**). On ceramic materials, however, such studies are rare and are confined to testing the static fracture properties under multiaxial loading conditions (**3–5**).

Depending on their application (in turbines or in motor parts or in chemical plants), ceramic parts may be stressed under different multiaxial loading conditions. As ceramics are brittle and have low tensile strengths, tensile loading in constructions containing ceramic parts is avoided as far as possible. No studies on the fatigue behaviour of ceramic materials under such loading conditions exist to the authors' knowledge until now. In metallic materials a

*University of Agriculture, Institute of Met. and Physics, Türkenschanzstr. 18, A-1180 Vienna, Austria.
†Technical University Vienna, Institute of Applied and Technical Physics, Karlsplatz 13, A-1040 Vienna, Austria.

drastic reduction of the fatigue crack propagation rates has been detected owing to the 'sliding mode crack closure' (sliding crack face interference), which is increased by compressive loads (**6**). The near-threshold fatigue crack growth behaviour of notched metallic specimens has been determined in a similar way with a superimposed constant torsional load (**7**). It has been found that the thresholds are shifted towards higher values, with increasing static loads and that sliding mode crack closure is the reason for this.

Another typical difference between ceramic and metallic materials is the poor plastic deformation capability and steep crack growth curve of ceramics. The low-cycle fatigue behaviour is then of less interest than high-cycle fatigue experiments, at least at room temperature. Therefore, experimental results from high-cycle fatigue experiments on plain tube specimens of zirconium oxide under cyclic torsion and superimposed compression load at room temperature are reported in this study. In order to reduce the testing times, a new ultrasonic fatigue testing device for cyclic torsional loading (**8**) has been further developed for biaxial loading conditions.

2 Experimental Details

2.1 *Biaxial fatigue machine*

In order to perform biaxial loading under static compression and cyclic torsional stresses, two loading systems have been combined:

(1) a conventional servohydraulic testing machine to generate constant compression loads;
(2) an ultrasonic torsion fatigue machine operating at a frequency of 20 kHz (**8**). This equipment is shown schematically in Fig. 1 with a tube specimen mounted. It is briefly described in the following.

A piezoelectric transducer generates torsional ultrasonic vibrations which form a standing torsional wave if the vibrating parts (mounting part I – amplification horn – specimen – mounting part II) are designed adequately. The specimen is subjected to this torsional vibration with a frequency of 20 kHz which produces cyclic stresses with a zero mean torsional stress ($R = -1$). The cyclic torsional stress amplitude is maximum in the centre of the specimen, decreases sinusoidally with increasing distance from the centre and becomes zero at the specimen ends.

Not only tube specimens but also compact plain cylindrical specimens can be tested with this method. In this case it is useful to test hourglass-shaped specimens instead of cylinders in order to amplify the torsional cyclic loads in a similar way as in tension–compression tests with ultrasound (**9**).

As shown in Fig. 1, several vibration nodes (zero displacement) are formed along the whole system. Two nodes of the system are used to introduce constant or slowly changing forces to the system and to perform biaxial loading conditions of the specimens. As shown in Fig. 1, the force of the actuator of the hydraulic machine is transduced via mounting part II to the specimen and the vibration

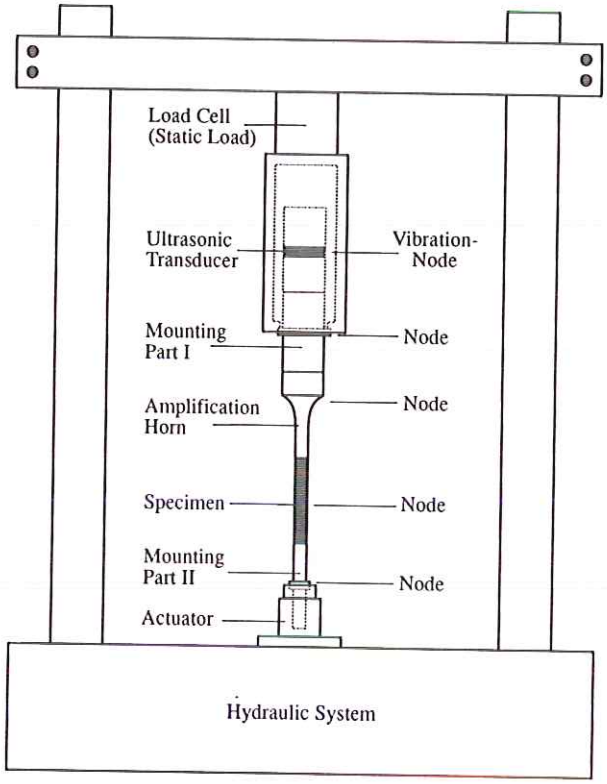

Fig 1 Schematic view of the biaxial testing machine for cyclic torsional loading (20 kHz ultrasound testing machine) plus superimposed constant compressive loading (hydraulic system).

of the ultrasonic transducer is transmitted via mounting part I and amplification horn to the specimen. The engineering of the load train must be such that the vibration system has two free ends. This means that the upper end is the ultrasonic transducer and the lower end is the free end of mounting part II. For fatigue tests under uniaxial torsional loading, mounting part II is not needed and the specimen is attached to the amplification horn only.

Static or slowly changing compressive forces (or tension–compression or tensile loads) are measured with a load cell placed in the load train of the hydraulic machine. The cyclic torsional load is measured in the centre of a specimen with micro-strain gauges. These measurements serve to calibrate and control the load amplitude during testing. Control of the torsional fatigue load is performed with a contact-free electromagnetic gauge which measures the torsional displacement at one specimen end where it is maximum. Displacement amplitudes at the specimen ends and strain as well as stress amplitudes in the centre of the specimens are directly proportional to each other so that the displacement amplitudes are used to control load amplitudes.

The specimen compliance increases after crack initiation and therefore the resonance frequency of the system decreases. A frequency control unit guarantees that loading frequency and resonance frequency of the torsional vibrator are equal. Detuning of the resonance system on the other hand is used to detect specimen failure and to switch off the machine automatically. More details especially on mounting parts I and II, amplification horn, specimen dimension, cyclic monitoring, calculation of torsional amplitudes from electric signals of the gauges and control of the ultrasonic system are described in more detail in (**8**, **9**).

2.2 *Material specimen geometry and testing procedure*

Specimen material was commercially produced zirconium oxide with nominally 99% ZrO_2. The density, ρ was 5.2 g/cm^3, the grain size 30–50 μm. The mechanical properties are: compression modulus of elasticity: 160 GPa, shear modulus: 65 GPa, Poisson's ratio: 0.23. The material was received as tubes with an outer diameter of 10 mm and an inner diameter of 6 mm. Specimen length (tube length), L_R was 88.5 mm. This length is determined by the resonance condition for cylindrical specimens under torsional vibration (**8**) from:

$$L_R = \frac{1}{2f_R} \cdot \sqrt{\frac{G}{\rho}}$$

with f_R = loading frequency and G = shear modulus. Care must be taken that the areas of the specimen ends are plain and smooth and exactly vertical to the tube axis, so that coupling of amplification horn and mounting part is perfect. Testing temperature was 20–22°C and relative humidity was 50–60%.

In order to characterize the fatigue behaviour of the material, S/N curves have been determined in the high cycle range of 10^5 to 10^9 cycles. As a characteristic fatigue strength parameter, the cyclic torsional amplitude $\Delta\tau/2$ has been used. In addition, S/N curves were measured with a rather small superimposed static compressive load σ_c of -25 MPa.

3 Results

3.1 *Fractography*

Figure 2 shows a specimen which broke under biaxial loading conditions, with a compressive stress, $\sigma_c = -25$ MPa, and a cyclic torsional stress amplitude, $\Delta\tau/2 = 72$ MPa. The fatigue crack initiates at an angle of approximately 45° to the specimen axis and propagates helically. This crack initiation behaviour has been observed on specimens which were cycled with a torsional load with and without superimposed static compression load. The crack propagation angle varies to some extent, but is not significantly different in specimens which were loaded with and without compressive pre-load. This means that the cracks propagate approximately in the planes of maximum principal stresses and are

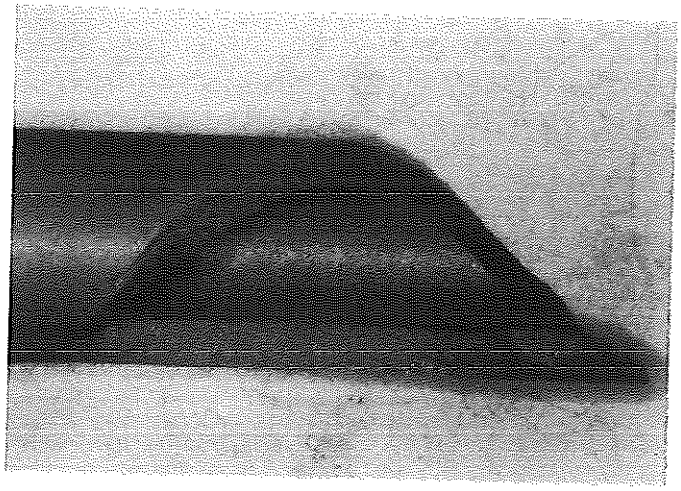

Fig 2 Specimen which has been broken by cyclic torsional plus superimposed static compressive loading.

mode I cracks. All observed fracture surfaces after uniaxial and biaxial loading show the features which are typical for torsional fatigue fractures of hard materials (**10**).

In addition to these 45° cracks, other cracks were also found, which propagated parallel to the tube axis. However, these cracks did not form during fatigue loading but during final fracture, as experimentally determined with a cracked but not completely fractured specimen.

3.2 *Fatigue crack characterization*

The fatigue data are summarized in S/N diagrams with the torsional amplitude on the y-axis for cyclic torsional loading with and without compressive pre-load as shown in Fig. 3.

A rough evaluation of the results shows that the number of cycles to failure (lifetime) increases by superposition of a compressive load in the low-cycle range by one order and in the high-cycle range by two orders of magnitude.

The S/N curves show neither a pronounced fatigue limit for pure cyclic torsion, nor for cyclic torsion plus superimposed static compression loading. If the torsional fatigue amplitude, $\Delta\tau/2$ is 55 MPa the lifetime of the specimens is more than 10^9 cycles which may be considered as a fatigue limit in a technical sense. This value increases to 62 MPa if a static compressive load of -25 MPa is superimposed.

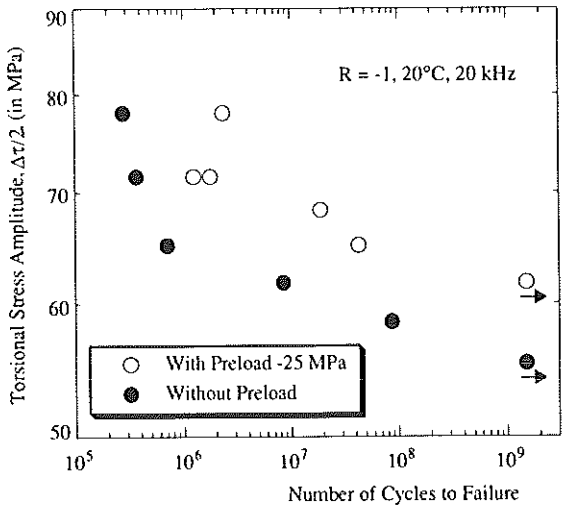

Fig 3 S/N curve of ZrO_2 for pure cyclic torsional loading and for cyclic torsional plus superimposed static compressive loading; y-axis: $\Delta\tau/2$ = cyclic torsional amplitude.

4 Discussion

The torsional fatigue system described is time and energy saving, with advantages and disadvantages discussed in the following.

Owing to the resonance vibration of the system, the torsional stress amplitude varies sinusoidally along the specimen length, with a maximum in the centre of the specimen. This stress distribution which is typical for high-frequency resonance loading systems means that the cyclic torsional stresses are almost zero within the coupling parts at the ends of the specimens. This is of great advantage especially if brittle materials with their brittle coupling parts (like clamps or screws) are tested.

The concentration of the maximum stress in the centre of the specimen is advantageous in high temperature studies as the desired testing temperature has to be maintained only in this part of the specimen.

The concentration of the stress amplitude at the centre of a specimen may have drawbacks in some cases. For example if materials with surface or volume defects (like pores) are studied, stressing of larger volumes is desirable in order to allow a better statistic evaluation of the influence of these defects on the fatigue properties (9).

However, in notched or pre-cracked specimens the loaded specimen volume is respectively restricted to the area around the notch or the crack tip. Therefore the non-constant stress along the specimen length does not play a role, so that the described testing method is appropriate for crack propagation studies.

The above-mentioned specimen dimensions are appropriate for 20 kHz ultrasound torsional vibrations in resonance. The resonance specimen length is approximately 60% longer for longitudinal vibrations than for torsional vibrations. Therefore the longitudinal waves cannot vibrate in resonance in the specimens designed for torsional resonance waves even if longitudinal vibrations were produced in addition to the desired torsional vibrations by the transducer. Thus undefined superimposed axial loads need not be considered. This testing system is not only time saving but also energy saving: a relatively small transducer (with low energy consumption) is necessary to obtain the required torsional stress amplitudes under resonance conditions.

The very high loading frequency makes possible a drastic reduction of the testing time. For example, 10^9 cycles are obtained within one day with the ultrasound fatigue machine whereas approximately one year is needed with a conventional machine.

The following facts, however, have to be observed more or less depending on the test material.

(i) Owing to the high loading frequency, much energy is pumped into the specimen within extremely short times. So certain metallic or polymeric specimens, for example, might be heated up too much. By introducing periodic pauses in between the load pulses, this heating-up of a specimen is avoided. In addition, cooling with pumped air or liquids is necessary in some cases. No significant heating was registered in the fatigue tests of this study with ceramic materials as the load amplitudes were rather low and the tested material is brittle.

(ii) If the material is insensitive to environmental influences, that is if no time-dependent effects are present, their fatigue behaviour may be determined with high as well as with low-frequency testing machines. If not only cycle-dependent but also time-dependent effects play a role, as in ceramic materials, the testing frequency must be considered adequately (**11**). Performing fatigue tests at the very high frequency of 20 kHz makes it possible to separate these two effects by assuming that time-dependent effects are reduced and that mainly cycle-dependent effects play a role. Therefore, the high-frequency testing machine is considered as a very effective time- and energy-saving method to determine the fatigue properties of some materials.

In addition, ceramic materials are eventually loaded in-service with frequencies in the ultrasonic range, for example, electric equipment with electrical resonances or turbines or motor parts. Therefore, fatigue data which have been obtained at ultrasonic frequencies are not only interesting from a material/scientific standpoint but also for engineering purposes.

The studies on zirconium oxide as presented in this paper are the first investigations on biaxial loading with an ultrasonic torsional fatigue system. No statistical evaluation of fatigue tests at identical cyclic torsional amplitudes has been performed. It may be concluded from the small scatter in the S/N data (Fig. 3) however, that the material behaviour is fairly well characterized by these measurements.

Figure 3 shows that the lifetime (number of cycles to fracture) as a function of the torsional stress amplitude, $\Delta\tau/2$ increases by superposition of a constant compressive load by several orders of magnitude in the high-cycle range. It may be concluded from the fracture surfaces that not the cyclic torsional load but rather the resulting tension–compression load in the direction of the principal normal stress determines the crack initiation process.

In order to discuss the influence of mean loads on the cyclic tension–compression behaviour, plotting the maximum tensile loads instead of the torsional amplitudes versus number of cycles to fracture, seems useful in analogy to tension–compression loading (**12**). Without preload, the maximum tensile stress, $\sigma_{T,\max}$ is effective under 45° to the specimen axis and its value is τ. If a compression stress, $\sigma_c = -25$ MPa, is superimposed on the cyclic torsional stress, the maximum value of the principal tensile stress $\sigma_{T,\max}$ is reduced to the value

$$\sigma_{T,\max} = \frac{\sigma_c}{2} + \sqrt{\left(\frac{\sigma_c}{2}\right)^2 + \tau^2}$$

The influence of maximum tensile stress $\sigma_{T,\max}$ on the number of cycles to fracture with and without preload is plotted in Fig. 4. The lifetimes are different for pure torsional and torsional plus superimposed compressive loading conditions, especially in the high-cycle range. Higher compressive stresses lead to *reduced* lifetimes in this kind of plot which is in contrast to the results in Fig. 3 with $\Delta\tau/2$ on the y-axis. This shows the damaging influence of a superimposed compressive load. A similar result has been obtained for tension–compression cyclic loading with different mean values (**13**).

With compression preload, the angle between principal stress and specimen axis changes from 45° to ϕ.

$$\tan(2\phi) = \frac{2\tau}{\sigma_c}$$

For a typical torsional stress amplitude in the range of 70 MPa and a compression preload $\sigma_c = -25$ MPa, an angle $\phi = 50°$ results. Assuming that the crack growth plane is oriented vertical to the planes of maximum tensile strength, the angle of 45° between specimen axis and crack plane for pure torsional loading would be reduced to approximately 40° for torsional loading with a superimposed compression load of −25 MPa. This small change, however, could not be detected unambiguously in this study as mentioned in paragraph 3.1.

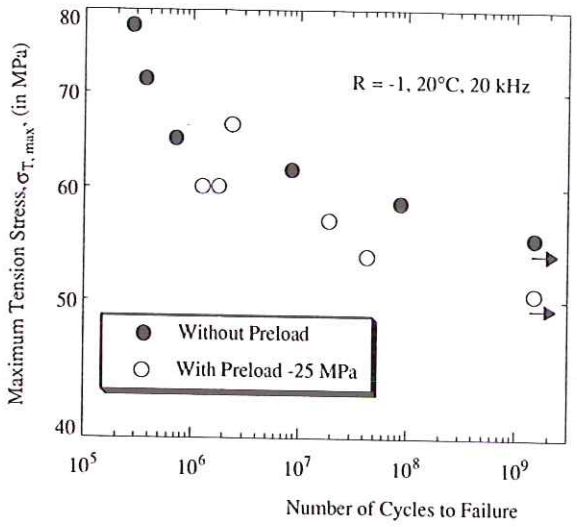

Fig 4 Same as Fig. 3, but with $\sigma_{T,max}$ = maximum value of the tensile part of loading, on the *y-axis*.

Possible micromechanisms of fatigue crack initiation and propagation have been discussed for monolithic fine-grained ceramics in several review papers (**12–16**). These studies mainly treat cyclic tensile or cyclic tensile plus compression loading. Crack initiation and propagation under torsional fatigue loading with and without superposition of tensile or compressive loads have not been discussed so far. As shown in this paper, crack initiation during high-cycle torsion fatigue loading takes place in mode I. Therefore, the models described in (**12–16**) should be appropriate to characterize the cracking behaviour under torsional loading as well. This question is examined by light and scanning electron microscopy in another study.

5 Conclusion

Tube specimens (outer diameter 10 mm, inner diameter 6 mm) of zirconium oxide have been fatigued under torsional loading conditions (loading frequency 20 kHz) with a superimposed static compression load in the high-cycle range (10^5 to 1.5×10^9 cycles) with a new time and energy saving device. The following results have been obtained.

(1) The fatigue behaviour (S/N curve, da/dN vs. ΔK curves, etc.) of ceramic materials can be characterized with the described ultrasonic torsion fatigue equipment under biaxial loading conditions. The described method is appropriate for near-threshold fatigue crack growth measurements under mode II (tube specimen with radial notch) and mode III (cylindrical specimen with circumferential notch) loading with and without superimposed static or slowly changing cyclic loads.

(2) The S/N curves for pure cyclic torsion and for cyclic torsion with superimposed static compression load do not have a fatigue limit. If the torsional amplitude, $\Delta\tau/2$ is 55 MPa, the number of cycles to fracture is higher than 10^9 cycles which may be considered as a "fatigue limit" from a technical point of view. If a static compressive load of -25 MPa is superimposed on the torsional fatigue load the "fatigue limit" increases to 62 MPa. Superposition of static compressive loads increase the lifetimes by 1–2 orders of magnitude.

(3) Crack initiation takes place in mode I and the fracture area is inclined approximately 45° towards the specimen axis under pure cyclic torsion and cyclic torsion plus superimposed compressive load.

(4) If the cyclic principal normal stress amplitude $\sigma_{T,\max}$ instead of the torsional amplitude, $\Delta\tau/2$ is plotted in an S/N diagram for pure torsional and for superimposed loading conditions, the curve is shifted towards *shorter* lifetimes for the superimposed loading condition. This result points to damage of the material during the compressive part of cycling.

Acknowledgements

The authors gratefully acknowledge financial support of this study by the Bundesministerium für Wissenschaft und Forschung, Wien. We also thank Mr. W. Laube for technical assistance.

References

(1) MILLER, K. J. and BROWN, M. W. (Editors) (1985) *Multiaxial Fatigue* ASTM STP 853, ASTM, Philadelphia PA 19103.

(2) KUSSMAUL, K. F., McDIARMID, D. L. and SOCIE, D. F. (Editors) (1991) *Fatigue under Biaxial and Multiaxial Loading*, ESIS Publication 10, Mechanical Engineering Publications Limited, London.

(3) SURESH, S. and TSCHEGG, E. K. (1987) Combined Mode I–Mode II fracture of fatigue – precracked alumina, *J. Am. Ceram. Soc.*, **70**, (10). pp. 726–33.

(4) SINGH, D. and SHETTY, D. K. (1989) Fracture of polycrystalline ceramics in combined Mode I and Mode II loading, *J. Am. Ceram. Soc.*, **71**, (1), pp. 78–84.

(5) SURESH, S., SHIH, A., MORRONE, A. and O'DOWD, (1990) Mixed-mode fracture toughness of ceramic materials, *J. Am. Ceram. Soc.*, **73**, (5), pp. 1257–67.

(6) TSCHEGG, E. K. (1983) Static Mode I and R-ratio influence on the Mode III fatigue crack behaviour in mild steel, *Mat. Sci. Engng.*, **59**, pp. 127–137.

(7) TSCHEGG, E. K., MAYER, H. R., CZEGLEY. M and STANZL, S. E. (1991) Influence of a constant Mode II load on Mode I fatigue crack growth thresholds, in *Fatigue under Biaxial and Multiaxial Loading*, (ed. by Kussmaul K. F., McDiarmid, D. L. and Socie, D. F.,) ESIS Publication 10, Mechancial Engineering Publications Limited, London, pp. 213–222.

(8) STANZL-TSCHEGG, S. E., MAYER, H. R. and TSCHEGG, E. K. (1993) High frequency method for torsion fatigue testing, *Ultrasonics*, **31**, (4), pp. 275–280.

(9) STANZL-TSCHEGG, S. E., MAYER, H. R., TSCHEGG, E. K. and BESTE, A. (1993) In-service loading of AlSi11 cast aluminium alloys in the very high-cycle regime, *Int. J. of Fatigue*, **15**, (4), pp. 311–316.

(10) TSCHEGG, E. K. and S. E. STANZL (1988) The significance of sliding crack closure on Mode III fatigue crack growth, *ASTM Symposium on Fundamental Questions and Critical Experiments on Fatigue*, Texas, Oct. 1984. ASTM STP 924, pp. 214–232.

(11) YOKOBORI TOSHIMITSU, ADACHI, T., YOKOBORI TAKEO, ABE, H., TAKAHASHI, H., NAKAYAMA, J. and FUJITA HIROYKI (1990) Time dependent and cyclic dependent effects of alumina ceramics under cyclic fatigue conditions, *J. of Ceramic Soc. of Japan*, **98**, (961), pp. 9–15.
(12) KISHIMOTO, H. (1991) Cyclic fatigue in ceramics, *JSME Intern. J., Series I*, **34**, (4), pp. 393–403.
(13) WEDDINGEN, A. and GRATWOHL, G. (1993) Ermüdung keramischer Werkstoffe, in: *Mechanische Eigenschaften keramischer Konstruktionswerkstoffe*, (Ed. G. Grathwohl) DGM.
(14) EVANS, A. G. (1980) Fatigue in ceramics, *Intern. J. Fracture*, **16**, (6), pp. 485–498.
(15) RITCHIE, R. O. (1988) Mechanism of fatigue crack propagation in metals, ceramics and composites: role of crack tip shielding, *Mater. Sci. Eng.*, **103**, (1), pp. 15–28.
(16) GRATWOHL, G. (1988) Ermüdung von Keramik unter Schwingbeanspruchung, *Mat.wiss. u. Werkstofftechn*, **19**, pp. 113–124.